PASSIVE MICROWAVE OBSERVATIONS OF THE HISTORIC FEBRUARY 2010 SNOW STORMS IN THE BALTIMORE/WASHINGTON D.C. AREA

James Foster [a], Gail Skofronick-Jackson [a], Huan Meng [b], George Riggs [a], Ben Johnson [a], Jim Wang [a], Dorothy Hall [a], Son Nghiem [c]

[a]NASA/ Goddard Space Flight Center, Hydrospheric and Biospheric Processes Laboratory

[b]NOAA/National Weather Service

[c]Jet Propulsion Laboratory

KEY WORDS: snowfall, historical, microwave, AMSR-E, AMSU-B

- -

ABSTRACT

The unprecedented snowfall during early February 2010 in the Baltimore/Washington area provided a unique opportunity to map, monitor and measure snowfall, snow cover extent, snow water equivalent (SWE), and snow melt using a suite of remote sensing instruments. Because snow cover in the Middle Atlantic area is in most years patchy and a true multi-layered snow pack is rarely established, utilizing a remote sensing approach to observe snow parameters is more challenging than in regions where falling snow and snow packs are more reliable. The Advanced Microwave Scanning Radiometer (AMSR-E) and Scanning Microwave/Instrument (SSM/I) data were used to assess SWE and the onset of melt. For this investigation, the Advanced Microwave Sounding Unit-B (AMSU-B) images were employed to detect falling snow. Snowfall observations and retrievals show that indeed falling snow signatures can be seen in high frequency brightness temperatures. Detection of falling snow is performed operationally, while retrieving falling snow rates is a new area of scientific research and still requires additional investigation. However, it is encouraging that, in general, where falling snow is occurring, on the surface below, snow cover is present.

Pixels that are mixed with water seriously compromise the efficacy of snow pack observing sensors operating in the microwave portion of the electromagnetic spectrum. The Chesapeake Bay and its wide mouthed, tidewater tributaries thus negatively impacts efforts to derive SWE and snowmelt. Furthermore, the average daytime maximum temperatures in this region are well above freezing, and on occasion even the daily minimum temperatures may remain above 0º C, confounding the passive microwave algorithms used to derive SWE, which assume dry snowpack conditions. Although the passive microwave signatures illustrated in this study are clearly related to snow, it's not straightforward whether or not the signatures are due to variations in SWE or to snowpack metamorphism or to a combination of both.

1 INTRODUCTION

The unprecedented snowfall during early February 2010 in the Middle Atlantic region, especially the area between central Virginia to northern Maryland, provided a unique opportunity to map, monitor and measure snowfall, snow cover extent, snow water equivalent (SWE), and snow melt in a typically challenging region, using a suite of remote sensing instruments. Because snow cover in the Middle Atlantic area is in most years patchy and a true multi-layered snow pack is rarely established, utilizing a remote sensing approach to observe snow parameters is more challenging than in regions where falling snow and snow packs are more reliable. Additionally, pixels that are mixed with water seriously compromise the efficacy of sensors operating in the microwave portion of the electromagnetic spectrum. The Chesapeake Bay and its wide mouthed, tidewater tributaries thus negatively impacts efforts to remotely estimate snow water equivalent and snowmelt. Furthermore, the average daytime maximum temperatures in this region is well above freezing and on occasion minimum temperatures may remain above 0º C, confounding the passive microwave algorithms used to derive SWE, which assume dry snow pack conditions.

For this investigation, the Advanced Microwave Sounding Unit-B (AMSU-B) images were employed to detect falling snow, the Advanced Microwave Scanning Radiometer

(AMSR-E) and Scanning Microwave/Instrument (SSM/I) data were used to assess SWE and the onset of melt. Each of these sensors has its own set of limitations in observing either falling snow or snow on the ground, and none was specifically dedicated or designed to look at only snow. Nevertheless, each one is very near to the optimum frequencies/wavelengths required for observing snowfall, snow extent, SWE, and snowmelt.

The purpose of this paper is to assess the utility of these instruments in making measurements in a particularly challenging remote sensing environment, as described above, during a record setting snowfall period – perhaps a 1 in 200 year event.

2. BACKGROUND

February 2010 was the snowiest month ever recorded at nearly every meteorological station in Virginia, Maryland and Delaware and at numerous stations in New Jersey and North Carolina. Though a wet month, it was not exceptionally wet, but nearly all of the precipitation that fell in the region, fell as snow. Monthly precipitation (melted snow) at Washington Dulles International Airport (IAD) was 11.76 cm or approximately 7.75 cm above the 30-year mean, and at the Baltimore-Washington International (BWI) Airport, 10.54 cm was observed or approximately 3 cm above the 30-year mean.

Persistent cold together with the abundant snowfall permitted snow to remain on the ground throughout the month, at least on north- facing slopes and in areas away from buildings. For example, at BWI the average monthly depth was 28 cm, at Dulles it was 25 cm and at the Ronald Reagan Washington National Airport (DCA) it was 20 cm. The maximum snow depth at BWI and IAD was 86 cm and 66 cm, respectively.

Beginning on January 30, 2010, a series of east snow storms (nor'easters) and Alberta Clippers buried the Middle Atlantic region. Snowfalls in a number of locations exceeded 135 cm (54 inches) during the 17-day period from January 29-February 15. Based on the 30-year average for the Baltimore/Washington area these events well exceeded the expected snowfall during this 2 1/2 week period which is less than 10 cm (4 in). These falling snow events were quite variable in time and space as shown in Figure X where the melted accumulation time series for the 5-6 February 2010 storm is shown for the BWI and IAD airport ground stations.

The DCA snow total of 149 cm (55 in) measured through February 10 surpassed the previous snowiest winter mark set in 1998/1999. BWI and IAD easily broke their prior snowfall records, observing 203 cm and 196 cm (80 in and 77 in), respectively. Less than 5 cm of snowfall was recorded at these stations after February 10.

3. SENSORS

3.1 AMSU-B

Falling snow particles in atmospheric clouds tend to cause scattering of incident microwave energy (*Gasiewski*, 1993). Since most of the incident energy comes from the cosmic background, the scattering from snow particles typically produces a decrease in satellite-observed brightness temperatures with respect to cloud free or liquid water only clouds for channels in the 89-200 GHz frequency range. Thus these channels can be used to detect and estimate falling snow (Skofronick-Jackson et al., 2004; Ferraro et al., 2005; Chen and Staelin, 2003; Kim et al., 2008; Noh et al., 2009).

The AMSU-B sensor on the NOAA-15, NOAA-16, and NOAA-17 satellites, along with the Microwave Humidity Sounder (MHS), an upgrade of the AMSU-B, on the NOAA-18 and European MetOp satellites, provides a cross-track scanning passive radiometer (e.g., Ferraro et al., 2005). The channel resolution is ~15km at nadir and ~25km at the furthest scan angle. These instruments were designed to measure atmospheric water vapor using sounding channels at 183±1, 183±3, 183±7 GHz in conjunction with 89 and 150 GHz. Yet, these channels are also sensitive to falling snow and graupel particles in clouds. NOAA has an operational product that detects falling snow in contrast to liquid rain (http://www.osdpd.noaa.gov/ml/mspps/rainprd.html).
These products are archived and distributed through the National Environmental Satellite, Data and Information Service (NESDIS). NOAA also has a Global Snow Fall Rate experimental product found at the following http://www.osdpd.noaa.gov/ml/mspps/sfrprd.html webpage.

3.2. Passive Microwave Radiometry (SSM/I, SSMIS and AMSR-E)

Microwave emission from a snow layer over a ground medium consists of contributions from the snow itself and from the underlying ground. Both contributions are governed by the transmission and reflection properties of the air-snow and snow-ground boundaries, and by the absorption/emission and scattering properties of the snow layers (Chang et al., 1976, Weisman and Matzler, 1999; Foster et al., 2005). Snow crystals in snow packs essentially scatter part of the cold sky radiation, which reduces the upwelling radiation measured with a radiometer (Schmugge, 1980) in a manner similar to scattering from falling snow ice crystals. The deeper or more compact the snowpack, the more snow crystals are available to scatter the upwelling microwave energy.

The Advanced Microwave Scanning Radiometer (AMSR-E), on board the Aqua (EOS) satellite, was launched in 2002. It is the most recent addition to the passive microwave suite of instruments, sensing at 10.0 18.7, 36.5, and 89 GHz. AMSR-E snow pack products (Kelly et al., 2003, Kelly, 2009) are archived and distributed through the National Snow and Ice Data Center, and are available in the

Equal Area SSM/I Earth Grid (EASE-grid) projection (at a 25 km x 25 km pixel scale).

To convert SD to SWE, a density map in EASE-grid projection was produced by mapping the mean January through March density measurements from data sets of Brown and Braaten (1998) and Krenke (2004) to the Sturm et al. (1995) seasonal snow classification map. Further information of properties on different snow classes was reported by Sturm et al. (1995) and Foster et al. (2005). For more detailed information about the SSM/I, SSMIS and AMSR-E algorithms see Foster et al. (1997) and Kelly (2009).

4 RESULTS

4.1 Falling Snow Observations and Results

The images in Figure Y show the 150 GHz brightness temperatures for selected AMSU-B and MHS overpasses on 5-6 February 2010 over the Washington, DC region. The 150 GHz channel shows a strong response (cooling) when falling snow is present. This signal appears as a blue or green color in the 150 GHz images and represents a decrease in brightness temperature of 30 to 60 Kelvin below the background temperature of ~250K. In clear air, however, snow and ice covered land surfaces can have similar brightness temperatures as when falling snow exists.

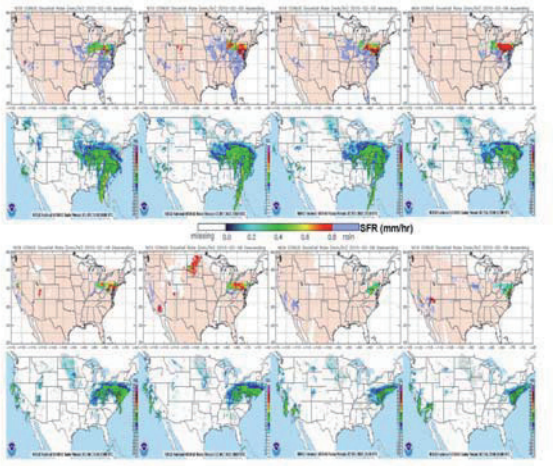

Figure 1
Falling snow retrieval results compared to the ground based NEXRAD radar mosaic images for 5-6 February 2010.

It is important to note that high variability exists in the AMSU-B images. The major contributor to the variability is obviously the falling snow and surface conditions within the field of view. Since these images are at overpasses near 0600, 1800, 2100, and 2300 UTC for 4-7 February 2010 the diurnal temperature conditions affect the surface temperatures dramatically and hence the emission from the surface, even though for these cases the temperatures remained below freezing. Another part of this variability is due to the cross-track scanning nature of the AMSU-B instrument that causes mixing of polarizations and slant path angles through the falling snow cloud profiles.

Brightness temperature maps for the AMSU-B 89 and 183±7 GHz channels show similar patterns as those appearing in the 150 GHz images (not shown). The 183±1 and 183±3 GHz channels are more sensitive to the water vapor in the vertical column and are decreasingly sensitive to falling snow the closer to the 183 GHz line center.

AMSU-B images have been compared with NOAA NEXRAD radar mosaic images to assess the capability of AMSU-B in detecting falling snow for the first major February snow event (Figure 1). AMSU-B and the radar images correspond surprisingly well for this storm sequence.

4.2. Snow Pack Observations and Results

The image sequences below (Figures 2 – 4) show selected SWE values for the period from January 31, the day after a 15 cm of snowfall across much of the area shown through March 3, when nearly all of the snow had melted. The biggest snows occurred on February 5/6 (Figure 2) and then again on February 9/10 (Figure 3). In early February there were problems with orbital gaps and or data not being acquired because of sensor problems. However, on the 7th and 8th, SWE values up to 60 mm (fuchsia color) in central and southwestern Virginia are evident. When comparing the AMSU-B 150 GHz image on 7 February (not shown) to the SWE image on the same day, the areas where SWE exist are cooler in the AMSU-B image. Where SWE is retrieved as zero, the AMSU-B brightness values are warmest. This is because without snow cover, the vegetation has a higher surface emission, resulting in warmer Tbs for both the AMSU-B and AMSR-E channels.

On February 6 and again on February 10, when heavy snow was falling; though, SWE is mapped, the values are negligible, despite the fact that well over 30 cm of snow cover the region, except for northern North Carolina and the tidewater area of Virginia. In cases of heavy snow falling in temperatures not far from 0º C, (rates > 2.5 cm/hour) the microwave signal in the AMSR-E channels is similar to that of falling rain – an absorption signal. In essence, the increase in Tb results in a SWE of zero.

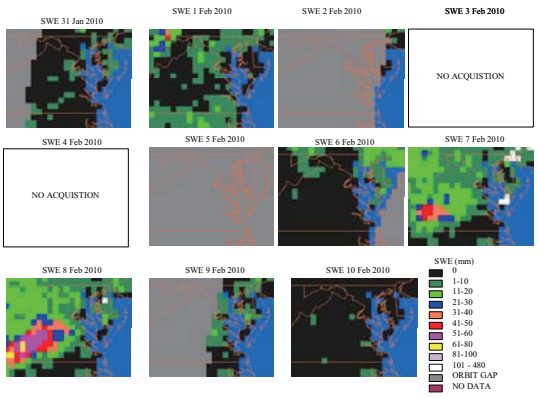

Figure 2
AMSR-E sequence from January 31 - February 10

Looking at the second panel, from February 11 – 20, it can be seen that, in general, much more SWE is being detected by the algorithm. Notice that again the most impressive SWE values are found in central and southwestern Virginia. In a few pixels, SWE values exceed 100 mm. However, in the Washington D.C. and Baltimore vicinity, SWEs are much more modest; < than 20 mm. It's well known that the presence of dense vegetation will act to increase Tbs, decreasing SWE, since the emissivity of trees can overwhelm the scattering of the underlying snow pack (Foster et a., 1991). The DC/Baltimore area has a considerable amount of tree cover but so do areas to the south and west where SWE values are highest.

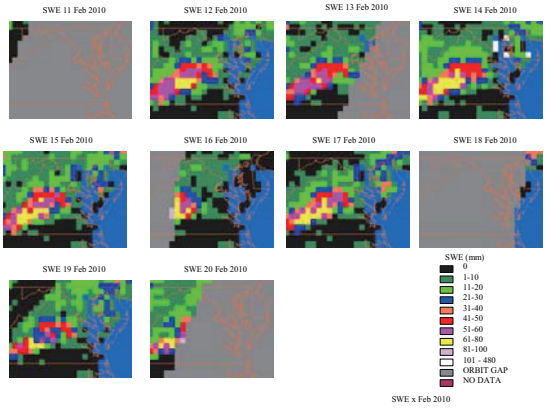

Figure 3
AMSR-E sequence from February 11 – February 20

It is also well understood that when the air temperature is at or above 0º C, the emissivity of the pack increases with a corresponding increase in Tb. Even 3% of liquid water will radically affect the imaginary portion of the dielectric constant of snow.

Note the panels for February 21, February 23 and 24 below. The snow pack; though melting, did not completely melt away as evidence by the panel for February 26. Rather above freezing temperatures ripened the pack, obscuring it from the AMSR-E sensor. The maximum temperatures at BWI on the 21st, 23rd and 24th were 8ºC, 6ºC and 7ºC, respectively. However, the minimum temperatures, near the time observed by AMSR-E, were -3º C, 2º C and 2ºC, respectively.

It is interesting that SWE is much more obvious in the metropolitan areas of Washington and Baltimore on the lower panels; February 21, February 26 and 28, for instance, than earlier in the month. The thickness of the pack did not suddenly increase here nor were the temperatures warmer here than in areas to the south and west where the SWE values were greatest.

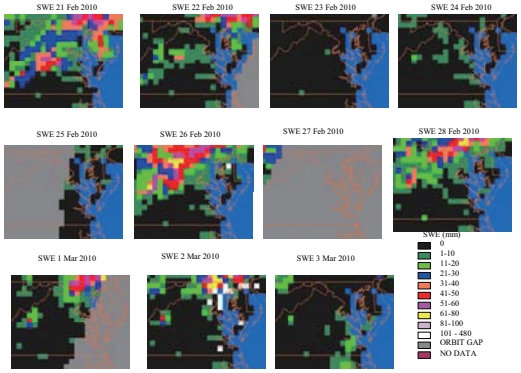

Figure 4
AMSR-E sequence from February 21 – March 3

5 DISCUSSION and CONCLUSIONS

Looking at temperature data for IAD, BWI, DCA, CHO (Charlottesville), ROA (Roanoke), and Hagerstown, there is no obvious warming or cooling that would explain the early month high SWE signatures in central and southwestern VA and the coincident lower SWE signatures in northern VA and central MD. Snow depths and corresponding SWE values were greater in the latter area than in the former. Vegetation differences are minimal across the piedmont area of VA and MD, and RFI is thought to play no role at all in either the differences in the SWE patterns or in the amounts.

Differences in crystal characteristics might either suppress or boost SWE values, but it is unlikely that changes in crystal structure are indeed confounding the algorithm to the degree illustrated. Nor is the large footprint size of the AMSR-E 10.7 GHz channel (51 x 29 km) likely a contributing factor – resulting in mixed land and water pixels. Nonetheless, SWE values in northern Virginia and central Maryland are suppressed in early to mid February when a deep snow pack is in place and are buoyed later in the month and in early March when the pack has largely melted.

Notice that the band of greater SWE values migrates from southwest to northeast during the course of the month. Again, this pattern does not seem to be following

temperature or precipitation trends. By March 2(Figure 4), extremely high SWE values are observed in the immediate Baltimore/Washington vicinity. At this time, though, the maximum temperatures were above freezing, and for most exposures snow no longer covered the ground.

Snowfall observations and retrievals show that indeed falling snow signatures can be seen in high frequency brightness temperatures. While retrieving falling snow rates is a new area of scientific research and still requires additional investigation, it is encouraging that, in general, where falling snow is occurring, on the surface below, snow cover is present.

In regard to snow on the ground, pixels that are mixed with water seriously compromise the efficacy of snow pack observing sensors operating in the microwave portion of the electromagnetic spectrum. The average daytime maximum temperatures in this region are well above freezing, and on occasion even the daily minimum temperatures may remain above 0º C, confounding the passive microwave algorithms used to derive SWE, which assume dry snowpack conditions. Although the passive microwave signatures in this investigation are clearly related to snow, it's not straightforward whether or not the signatures are due to variations in SWE or to snowpack metamorphism or to a combination of both.

Acknowledgements

CLASS data system for AMSU-B data.

References

Brown, R. and R. Braaten, 1998, Spatial and temporal variability of Canadian monthly snow depths, 1946-1995. *Atmosphere-Ocean*, Vol. 36(1), 37-45.

Chang, A.T.C., Gloersen, P., Schmugge, T., Wilheit, T., and Zwally, J., 1976, Microwave emission from snow and glacier ice. J*ournal of Glaciology,* 16: 23-39.

Chen F. W. and D. H. Staelin (2003), AIRS/AMSU/HSB precipitation estimates, *IEEE Trans. Geosci. Remote Sens.*, *41*, 410-417.

Ferraro R. R., F. Weng, N. C. Grody, L. Zhao, H. Meng, C. Kongoli, P. Pellegrino, S. Qiu, and C. Dean, (2005), NOAA operational hydrological products derived from the advanced microwave sounding unit. *IEEE Trans. Geosci. Remote Sens.*, *43*, 1036-1049 .

Foster, J.L., A.T.C. Chang, and D.K. Hall, 1997, "Comparison of snow mass estimates from a prototype passive microwave snow algorithm, a revised algorithm and a snow depth climatology," *Remote Sens. Environ.*, 62, 132-142.

Foster, J., Sun, C., Walker, J., Kelly, R., Chang, A., Dong, J., and Powell, H., 2005, Quantifying the uncertainty in passive microwave snow water equivalent observations. *Remote Sensing of the Environment,* 94:187-203.

Gasiewski, A. J. (1993), Microwave radiative transfer in hydrometeors, in *Atmospheric Remote Sensing by Microwave Radiometry*, edited by M. A. Janssen, pp. 91-144, John Wiley and Sons, New York.

Kelly R.E.J., Chang, A.T.C., Tsang, L., and Foster, J.L., 2003, A prototype AMSR-E global snow area and snow depth algorithm. *IEEE Trans. Geosci. Remote Sens*., EO-1 Special Issue, 41 (2):230-242.

Kelly, R.E.J.,2009, The AMSR-E Snow Depth Algorithm: Description and Initial Results. *Journal of the Remote Sensing Society of Japan*.

Kim, M.-J., J. A. Weinman, W. S. Olson, D.-E. Chang, G. Skofronick-Jackson, and J. R. Wang (2008), A physical model to estimate snowfall over land using AMSU-B observations, *J. Geophys. Res.*, *113*, D09201, doi:10.1029/2007JD008589.

Krenke, A., 1998, updated 2004. Former Soviet Union hydrological snow surveys, 1966-1996. Edited by NSIDC. Boulder, CO, National Snow and Ice Data Center/World Data Center for Glaciology, Digital media.

NOAA, February 2010 temperature, precipitation and snowfall data for DCA, BWI, IAD, Charlottesville and Martinsburg.

Noh, Y.-J., G. Liu, A. S. Jones, and T. H. Vonder Haar (2009), Toward snowfall retrieval over land by combining satellite and in situ measurements, *J. Geophys. Res.*, *114*, D24205, doi:10.1029/2009JD012307.

Schmugge, T., 1980, Techniques and applications of microwave radiometry, in *Remote Sensing in Geology*, Siegal, B.S. and Gillespie, A.R. (eds), John Wiley, New York, Chapter 11, 337-352.

Skofronick-Jackson, G. M.-J. Kim, J. A. Weinman, and D. E. Chang (2004), A physical model to determine snowfall over land by microwave radiometry, *IEEE Trans. Geosci. Remote Sens.*, *42*, 1047–1058.

Sturm, M., Holmgren, J. and Liston, G.E., 1995, A seasonal snow cover classification system for local to regional applications. *Journal of Climate*, 8, 1261-1283.

Wiesman, A., and C. Mätzler (1999), Microwave emission model of layered snowpacks. *Remote Sensing of Environment,* 70, 307-316.